Applied Catalysis B: Environmental 117–118 (2012) 236–245

Contents lists available at SciVerse ScienceDirect

Applied Catalysis B: Environmental

journal homepage: www.elsevier.com/locate/apcatb

Gas-phase hydrodechlorination of trichloroethylene over Pd/NiMgAl mixed oxide catalysts

B.T. Meshesha[a], N. Barrabés[b], K. Föttinger[b,*], R.J. Chimentão[a], J. Llorca[c], F. Medina[a], G. Rupprechter[b], J.E. Sueiras[a]

[a] Department of Chemical Engineering, Universitat Rovira i Virgili, Campus Sescelades, 43007 Tarragona, Spain
[b] Institute of Materials Chemistry, Vienna University of Technology, Getreidemarkt 9 BC, 1060 Vienna, Austria
[c] Institut de Tècniques Energètiques, Universitat Politècnica de Catalunya, Diagonal 647, 08028 Barcelona, Spain

ARTICLE INFO

Article history:
Received 14 October 2011
Received in revised form 3 January 2012
Accepted 14 January 2012
Available online 24 January 2012

Keywords:
Hydrodechlorination
Trichloroethylene
Pd
NiMgAl mixed oxides
Ni Hydrotalcite

ABSTRACT

Hydrotalcite derived NiMgAl mixed oxide (NiHT) catalysts with different NiMgAl molar ratio were synthesized and tested in the selective gas-phase hydrodechlorination of trichloroethylene to ethylene. The mixed oxide was further promoted by Pd in order to obtain Pd/NiHT catalysts. The catalysts performances for hydrodechlorination of trichloroethylene depend on the Ni/Mg/Al molar ratio, reduction temperature, and method of noble metal incorporation. The main products obtained were ethylene, methane, ethane, chloroethylene and traces of dichloroethylene. The higher the Ni amount in the NiHT support was, the higher were the catalytic activity and ethylene selectivity. Introduction of Pd increases the catalytic activity. Application of higher reduction temperatures improved the selectivity towards ethylene formation due to an increase in the concentration of surface metallic Ni. A better Pd-Ni surface interaction was obtained by impregnation of Pd on a previously reduced (823 K) NiHT catalyst, resulting in higher ethylene selectivity (80%). The higher selectivity was associated to metallic Ni promoted by a Pd-Ni alloy, which was detected by HRTEM.

1. Introduction

Trichloroethylene (TCE) is one of the most widely distributed halogenated organic pollutants throughout the world. It is a volatile organic compound that has been used extensively as degreasing agent (in metals and rubber industry), dry cleaning agent and as a polymer precursor [1,2]. The primary environmental releases of trichloroethylene are due to air emissions from metal degreasing plants, and water from metal finishing and rubber processing industries. TCE could contribute to formation of photochemical smog and ozone depletion [1,3–5]. It has also been found out that TCE is a potent carcinogen [6] and resistant to natural degradation causing long-term environmental and health risks [5].

Catalytic hydrodechlorination (HDC) is a promising reductive technology that converts the organochlorinated pollutants into non-toxic, easily degradable or useful raw materials. It has been proposed as a treatment allowing the recovery of alkenes from undesired chloro-aliphatic compounds like TCE. However, in some cases, the concentration of TCE is very low in real gaseous emissions, i.e. gaseous emissions containing chlorinated compounds are diluted, often in air, which can introduce some limitations in the hydrodechlorination process. Therefore, a pretreatment (concentration of the substrate) of the gaseous emissions should be applied before the HDC reaction. For instance, concentration of TCE by certain carbon sorbents (like active carbon) can be applied prior to the HDC reaction [7]. When the concentration of TCE reaches a significant amount the hydrodechlorination process can be applied to produce useful products.

Most studies on HDC of TCE compounds have been carried out using noble metal catalysts [6,8]. Although supported noble metal catalysts, particularly Pd, exhibit good catalytic activities and stability during HDC of TCE at mild conditions, they mainly produce ethane, which is a much less desired product than ethylene [2,8,9]. There are reports that higher olefin selectivity can be attained by doping the noble catalysts with transition metals like Ag [9], Cu [2,10] or Sn [11]. For instance, supported bimetallic Pd-Cu or Pd-Ag catalysts are described to selectively hydrodechlorinate TCE to ethylene [5,9,10,2]. Another active transition metal catalyst is nickel, which is able to catalyze HDC of vicinal aliphatic chlorinated carbons. Ni catalysts studied for HDC of various aliphatic chlorinated compounds include: $NiMo/Al_2O_3$ [4,12,13], Ni/Al_2O_3[4,14], Ni/Zeolite [15], Ni/SiO_2 [4], Ni/AC [16,17] and Raney Ni [4,17]. Unlike noble metal catalysts, supported Ni catalysts have shown to be selective for ethylene production during HDC of vicinal

* Corresponding author. Tel.: +43 1 58801 165110; fax: +43 1 58801 16599.
E-mail address: karin.foettinger@tuwien.ac.at (K. Föttinger).

0926-3373/$ – see front matter © 2012 Elsevier B.V. All rights reserved.
doi:10.1016/j.apcatb.2012.01.018

chlorocarbons [16,18,19]. The major disadvantage of using Ni catalysts is that it requires high temperature (>473 K) or high hydrogen pressure to reach significant activity and that rapid catalyst deactivation occurs. Promotion of Ni rich catalysts using small amount of noble metals like Pd increases its catalytic activity for HDC reaction [20–22]. By this, it is possible to design Pd-Ni bimetallic catalysts being selective for olefin formation.

Moreover, the selection of an appropriate catalyst structure is important to modify the catalytic behavior (activity, selectivity and stability) and limit the degree of deactivation [9]. For instance, the choice of catalyst support and method of preparation can play an important role in the development of hydrodechlorination catalysts [18,23]. Lately, mixed oxides from hydrotalcite-like precursors containing noble metals are receiving attention for HDC reaction due to their numerous advantages for catalysis. These new catalytic materials inhibit deactivation by metal sintering, coking or poisoning by HCl produced during the HDC reaction [23]. Moreover, a clear effect of the basic properties of the supports has been reported on the catalytic properties for HDC reactions in which the Pd reactivity increases with higher Mg content in the Mg/Al hydrotalcite derived mixed oxide [23]. In gas-phase HDC of TCE Pd or Pt modified Cu/Mg/Al hydrotalcite derived mixed oxides have also shown improved catalytic activity, enhanced selectivity to ethylene and good stability [10]. HDC of 1,2,4-trichlorobenzene on Ni/Mg/Al hydrotalcite derived mixed oxide exhibited higher activities [24]. In general, incorporation of an active metal like Ni inside the hydrotalcite structure can favor the HDC activity, since the metal and the basic sites of Mg are in close proximity. Based on this, in the present work hydrotalcite derived NiMgAl mixed oxides with different Ni/Mg/Al molar ratios were prepared and consequently promoted by Pd. These catalysts were studied for gas-phase hydrodechlorination of trichloroethylene at 573 K. The influence of support composition and catalyst reduction temperature was studied. Previously, it was reported that immobilization of Pd over a pre-reduced CuMgAl catalyst showed Pd/Cu interaction (alloy formation), which was beneficial for the catalytic performance [10]. This preparation protocol was also studied for Pd supported on reduced NiMgAl catalysts. Several characterization techniques were employed in order to correlate physical–chemical properties and composition with the catalytic properties in the hydrodechlorination reaction.

2. Experimental

2.1. Catalysts synthesis

The Ni/Mg/Al (NiHT) and Mg/Al (HT) hydrotalcite were prepared by co-precipitation, as previously described [23]. Aqueous solutions of appropriate amounts of $Ni(NO_3)_2{\cdot}6H_2O$, $Mg(NO_3)_2{\cdot}6H_2O$ and $Al(NO_3)_2{\cdot}9H_2O$ salts and 3 M NaOH alkaline solution were separately prepared. These solutions were then simultaneously added drop-wise into 100 ml of deionized water maintaining a constant pH (10 ± 0.5) under vigorous mechanical stirring. After the co-precipitation, the suspension was aged overnight under stirring at room temperature, filtered, and thoroughly washed with deionized water. The resulting solid was then dried overnight at 373 K and calcined at 723 K for 15 h to obtain the hydrotalcite derived NiHT mixed oxides. In such a way, three different nickel mixed oxides (NiHT) with different molar ratios were synthesized, which are summarized in Table 1. These catalysts were labeled as NiHT1, NiHT2 and NiHT3, respectively.

Pd/NiHT and Pd/HT catalysts were prepared by impregnation of the mixed oxide with a toluene solution of Pd acetylacetonate, (Pd = 0.5 wt.%). The resulting catalysts were dried at 373 K and calcined at 623 K for 2 h. These catalysts were designated as Pd/NiHT1, Pd/NiHT2, Pd/NiHT3 and Pd/HT.

The NiHT1 sample was reduced at three different temperatures: 623, 723, and 823 K to study the effect of the reduction temperature and the samples were labeled as, for instance NiHT1-723 indicating the NiHT1 catalyst was reduced at 723 K.

For the introduction of Pd, another protocol was also studied. In this protocol, the NiHT1 mixed oxide was previously reduced at 823 K for 2 h. Then, the reduced sample (labeled as rNiHT1) was introduced into a toluene solution containing $Pd(AcAc)_2$. These steps were carried out under argon atmosphere in order to avoid re-oxidation of nickel. The solvent was then evaporated in vacuum, dried in 373 K and finally calcined at 623 K for 2 h. In this way, three Pd/rNiHT1 catalysts with different Pd weight percentage (0.5, 0.3, 0.1 wt.%) were prepared. The catalysts were designated as Pd(0.1)/rNiHT1, Pd(0.3)/rNiHT1 and Pd(0.5)/rNiHT1, respectively.

2.2. Catalysts characterization

Different characterization techniques were applied to study physico-chemical properties of the catalysts. The chemical composition of the samples was determined by atomic absorption spectroscopy with a PerkinElmer Plasma 400 instrument. N_2-physisorption was measured using a Micromeritics ASAP 2000 surface analyzer at 77 K. BET surface areas and average pore diameters were thus determined. Before analyses, all the samples were degassed in vacuum at 393 K for 12 h. The XRD analysis of the materials were recorded using a Siemens D5000 diffractometer (Bragg-Bentano parafocusing geometry and vertical θ–θ goniometer) fitted with a grazing incident (ω: 0.52°) attachment for thin film analysis and scintillation counter as a detector. The samples were dispersed on Si(5 1 0) sample holder. The angular 2θ diffraction range was between 5° and 90°. The data were collected with an angular step of 0.03° at 12 s per step and sample rotation. Cu Kα radiation (λ = 1.54056 Å) was obtained from a copper X-ray tube operated at 40 kV and 30 mA. The crystalline phases were identified using the JCPDS files.

The hydrogen chemisorption analysis was performed under static volumetric conditions with a Micromeritics ASAP 2010 apparatus. Prior to the measurement, the sample was evacuated at 373 K for 1 h, treated in flowing pure hydrogen (30 $cm^3\ min^{-1}$) at 623 K for 3 h, evacuated at 623 K for 1 h, cooled down to 373 K and evacuated 30 min. Finally, the chemisorption analysis was performed at 373 K. The double isotherm method was used to determine the amount

Table 1
Some properties of the catalysts.

Catalysts	Pd (wt.%)[a]	Ni/Mg/Al molar ratio[a]	BET surface area (m^2/g)	Pore diameter (nm)	D (%)[b]	H_2 uptake (cm^3/g)	dp (nm)[c]	TOF (s^{-1})[d]
Pd/HT	0.5	Mg_4Al_1	170	8.3	10	0.047	4.0	2.6
Pd/NiHT1	0.5	$Ni_{1.4}Mg_{0.7}Al_1$	115	9.9	19	0.1	4.1	1.3
Pd/NiHT2	0.54	$Ni_{0.75}Mg_1Al_1$	151	8.7	14	0.075	4.0	0.9
Pd/NiHT3	0.5	$Ni_{0.75}Mg_{3.1}Al_1$	146	10.3	5	0.026	4.3	4.4

[a] Obtained by atomic absorption spectroscopy.
[b] Pd dispersion obtained from H_2 chemisorption data.
[c] Pd particle size obtained from HRTEM.
[d] Turnover frequency values at 573 K.

of irreversibly adsorbed hydrogen, which allows calculating the apparent metallic dispersion (H/Pd) assuming an adsorption stoichiometry of H:Pd = 1:1. From the first isotherm, the total volume of hydrogen adsorbed was obtained. The sample was evacuated (about 10^{-6} mbar) again at the chemisorption analysis temperature for 10 min for back sorption measurements in order to obtain the volume of hydrogen reversibly adsorbed. The linear zone of each isotherm was extrapolated to zero pressure in order to estimate the volume of the strongly adsorbed hydrogen.

High-resolution transmission electron microscopy (HRTEM) was carried out with a JEOL 2010F instrument equipped with a field emission source. The point-to-point resolution was 0.19 nm and the resolution between lines was 0.14 nm. Samples were grounded and deposited on holey-carbon-coated grids from ultrasonicated alcohol suspensions. About 200–250 individual particles were used in each sample for particle size determination.

The temperature programmed reduction studies were performed in a ThermoFinnigan (TPORD 110) apparatus equipped with a thermal conductivity detector (TCD). The samples were then purged with argon flow before the TPR analysis. The analysis was carried out using a 3% H_2/Ar gas flowing at 20 ml min^{-1} by heating from room temperature to 1173 K with a ramp of 10 K min^{-1}. Water produced during TPR was trapped in CaO + Na_2O (soda lime) before reaching the TCD. The characterization results were used to interpret the catalytic properties.

2.3. Catalytic activity

The catalysts were tested for the gas-phase hydrodechlorination reaction of TCE using a continuous fixed-bed glass reactor described previously [9]. The reaction temperature was always kept at 573 K. The gas feed was obtained by an inert gas (He) and hydrogen flowing through a saturator kept at 298 K by a thermostat, containing liquid TCE. The TCE partial pressure was 92 mbar. The molar ratio of H_2/TCE was maintained at 3.5. The gas flows are adjusted by mass flow controllers (Brooks Instrument 0154) and introduced into the reactor, which is placed in a furnace coupled with a temperature controlling system. The outlet of the reactor is connected by a six-way valve to a gas chromatograph (HP 5890 series II, HP Poraplot column, FID). Catalytic conversion and selectivity were calculated by analyzing the peak areas of TCE and the respective products. For some catalysts, different space velocity was used to achieve lower conversion levels maintaining similar H_2/TCE molar ratio. All catalysts (100 mg) were reduced before to the start of the reaction by using pure hydrogen (20 ml min^{-1}) for 2 h. Turnover frequency, TOF (expressed in s^{-1}), values were calculated as the molecules of TCE converted per unit time (molecules of TCE s^{-1} g^{-1} catalyst) and per number of chemisorbed hydrogen atoms (atoms of H g^{-1} catalyst). The number of hydrogen atoms for each catalyst was calculated from the hydrogen chemisorption data.

3. Results

3.1. Characterization of the catalysts

Atomic composition and textural properties of the catalysts are summarized in Table 1. The atomic composition of Ni, Mg and Al showed small differences with respect to the initial molar ratios introduced during the preparation. N_2-physisorption results for the Pd/NiHT catalysts suggest that the difference in molar composition between Ni, Mg and Al affects the textural properties of the materials. Table 1 clearly demonstrates that the BET surface area of the NiHT catalysts is highly affected by the chemical composition of the sample. Pd/HT catalyst showed the highest surface area value (170 m^2/g). Comparing the catalysts containing nickel, Pd/NiHT2 possesses a higher BET surface area of 151 m^2/g. With increasing Ni content, the surface area decreased to 115 m^2/g for Pd/NiHT1. This is probably due the higher crystallinity of NiO. In addition, increasing the Mg content, as in Pd/NiHT3, moderately lowers the BET surface area to 146 m^2/g. X-ray diffraction patterns of the hydrotalcite derived mixed oxide catalysts (Pd/NiHT1, Pd/NiHT2, Pd/NiHT3) are shown in Fig. 1. After calcination at 723 K, the lamellar structure of the catalyst disappears and crystalline NiO phase is observed. The XRD profile for the Pd/NiHT samples did not reveal reflections corresponding to palladium species or $NiAlO_x$ spinel phase. As the Pd loading was rather low, the absence of diffraction lines of Pd may be due to the fact that the corresponding Pd particles are too small or highly dispersed [25] to be detected by XRD. The crystallinity of the catalysts was affected by the molar composition of the NiMgAl support. Pd/NiHT2 and Pd/NiHT3 showed a decrease in crystallinity, compared to the Pd/NiHT1 catalyst. The higher cystallinitiy and hence the lower BET surface area for Pd/NiHT1 catalysts is probably due to the segregation of NiO phase of the mixed oxide.

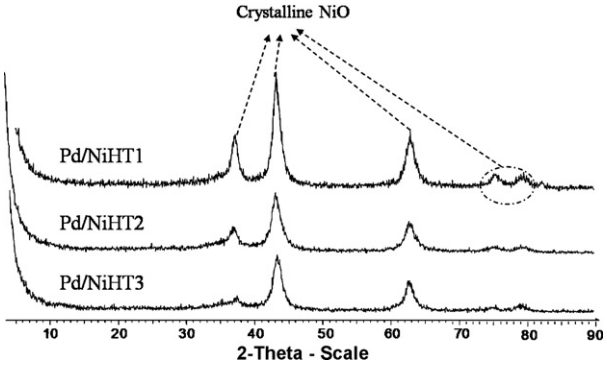

Fig. 1. X-ray diffraction patterns for the different Pd/NiHT catalysts.

The hydrogen chemisorption analysis for Pd/NiHT1, Pd/NiHT2, Pd/NiHT3 and Pd/HT catalysts was performed after reduction at 623 K. The hydrogen uptake results are shown in Table 1. The highest hydrogen uptake was recorded for Pd/NiHT1 catalyst (0.1 cm^3/g), while the lowest was observed for Pd/NiHT3 (0.026 cm^3/g). The hydrogen uptake capacities for the catalysts follow a trend: Pd/NiHT1 > Pd/NiHT2 > Pd/HT > Pd/NiHT3. The presence of a higher concentration of Pd-Ni enhances the H_2 uptake capacity, as shown for Pd/NiHT1 catalyst. On the other hand, the lower Pd-Ni concentration in the Pd/NiHT3 catalyst leads to poor hydrogen uptake. As also demonstrated in previous works, increasing the basicity by increasing the Mg/Al molar ratio favors more metal-support interaction decreasing the hydrogen uptake capacity [23]. This fact was also corroborated by the low hydrogen uptake observed for the Pd/HT catalyst. Hence, apart from the lower Ni content, the increase in Mg content can be responsible for the decrease in hydrogen uptake capacity.

The catalysts were further characterized using HRTEM and TEM techniques. A low-magnification, general TEM view of sample Pd/NiHT3 is shown in Fig. 2a. Hydrotalcite derived nickel mixed oxide support is comprised by homogeneous particles of about 5–10 nm in size. The support crystallites are well faceted and exhibit sharp edges, as deduced by the representative HRTEM image shown in Fig. 2d, which corresponds to the Pd/NiHT3 sample. In addition to support crystallites, the sample also contains round-shaped particles with a high electron contrast, which correspond to metallic Pd, as indicated in Fig. 2d. The distribution of Pd particles in this sample is very homogeneous and centered at about 4.3 nm, being most of them (>90%) comprised in the very narrow interval of 3–5 nm. The microstructure of the other two samples, Pd/NiHT1 and Pd/NiHT2, is very similar. Fig. 2b shows a representative image of sample Pd/NiHT1. Again, well-faceted support

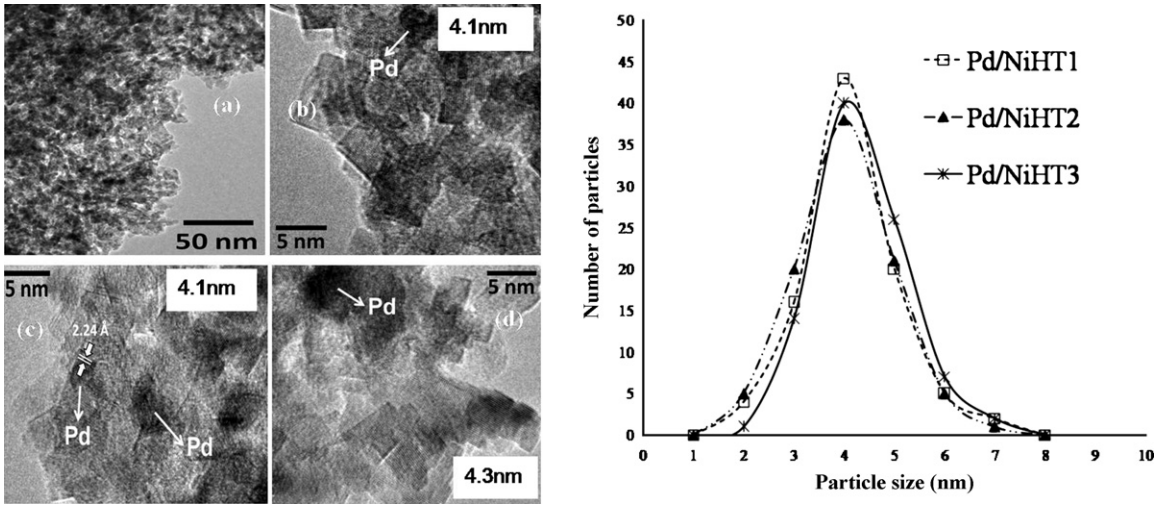

Fig. 2. HRTEM images of Pd/NiHT catalysts: (a) Pd/NiHT3; (b) Pd/NiHT1; (c) Pd/NiHT2; (d) Pd/NiHT3.

crystallites are homogeneously distributed in the sample along with smaller, round-shaped Pd particles. For this sample, the mean size of Pd particles is centered at about 4.1 nm. A similar situation is encountered in sample Pd/NiHT2 (Fig. 2c), where both the mixed oxide support and Pd particles exhibit virtually the same particle size distribution. In all cases, from HRTEM analysis of lattice spacing no evidence for the existence of Pd-Ni alloy or Pd covered by Ni has been encountered, although the groundmass of the support particles prevents an exhaustive and accurate analysis. However, in all cases where Pd lattice fringes are observed for instance in Fig. 2c at 2.24 Å for Pd(1 1 1), no evidence for covering has been observed. In addition, the spacing values determined correspond to pure Pd metal, thus suggesting that no alloy with Ni occurs.

Reducibility studies of NiHT and Pd-NiHT were performed by H_2-TPR. It is well known that supported metal catalysts show different reduction patterns depending on the nature of interaction with the support. The TPR profiles of NiHT catalysts are represented by dotted lines, as shown in Fig. 3. For NiHT catalysts, the reduction peaks of NiO are observed at relatively high temperatures (TPR peaks at > 798 K). They can be reasonably associated with the reduction of NiO that is incorporated into the framework or partially covered by the mixed oxide. The broad NiO reduction peaks of NiHT1, NiHT2, and NiHT3 are centered at 1013 K, 1058 K, and 1118 K, respectively. The comparison of the TPR profiles obtained for different NiMgAl samples showed that, upon increasing the Mg content, a shift of the NiO reduction peak towards higher temperatures and lower hydrogen consumption was observed. A shift to higher reduction temperatures of NiO in the presence of Mg is well documented in the literature [26], and it was associated to the formation of a NiO–MgO solid solution, in which Ni ions are stabilized against reduction and sintering by the MgO type matrix. Increasing the Ni content increased both the reducibility of NiO at lower temperature and the hydrogen uptake, as shown for NiHT1 catalysts. This is probably due to the high surface enrichment of NiO in the NiHT1 catalyst.

The solid lines in Fig. 3 represent the TPR profiles for Pd impregnated on NiHT catalysts. Separate reduction peaks of PdO at lower temperature and NiO at higher temperatures were observed. The TPR peaks between at 373 and 573 K are attributed to the reduction of PdO species with different interaction with the mixed oxide surface, as displayed in the inset of Fig. 3. In Pd/NiHT3 catalyst, the Pd reduction peaks are shifted to higher temperatures, whereas increasing the Ni content inside the mixed oxide facilitates the reduction of Pd at lower temperature, as shown for Pd/NiHT1 catalyst. In general, the reducibility of Pd over the NiMgAl mixed oxide depends on the strength of Pd interaction with different sites of the mixed oxide support. The TPR profiles illustrate that the presence of Pd affects the reducibility of NiO in all catalysts, which is demonstrated by the respective shift of the reduction peak of the NiO to the lower reduction temperature upon addition of Pd. Moreover, the hydrogen consumption of the NiO species increases as revealed by the increase in the peak intensities. Even though, the HRTEM study revealed no Pd-Ni alloy formation in all catalysts, it seems that there is surface interaction and cooperation between Pd-Ni, as demonstrated by the shift in reduction peaks and the change in peak areas in the TPR.

3.2. Catalytic properties in the hydrodechlorination of TCE

3.2.1. Influence of the support composition

The gas-phase HDC of TCE over Pd/NiHT catalysts (reduced at 623 K) was performed at 573 K. Different products were formed, such as chlorinated hydrocarbons, hydrocarbons, and HCl. The catalytic properties of Pd/NiHT and Pd/HT catalysts are shown in Fig. 4. The conversion against time of reaction is displayed in Fig. 4a. The catalytic activity was strongly dependent on the composition of the support. The Pd/HT, Pd/NiHT1 and Pd/NiHT3 catalysts showed higher initial TCE conversion (>80%) than the Pd/NiHT2 catalyst, which reached <60% conversion. This can be attributed to the metal-metal and metal-support interaction. When comparing the Pd/NiHT catalysts, the higher TCE conversion observed for Pd/NiHT1 catalyst could be related to its higher hydrogen uptake capacity resulting from the Pd-Ni interaction. Hence, the close contact of Pd and Ni on the catalyst surface is influential in the HDC

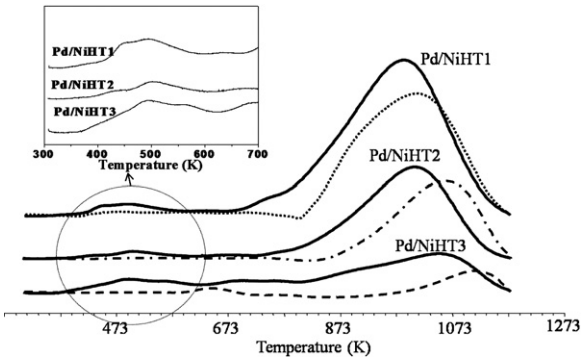

Fig. 3. TPR profiles for NiHT and Pd/NiHT catalysts.

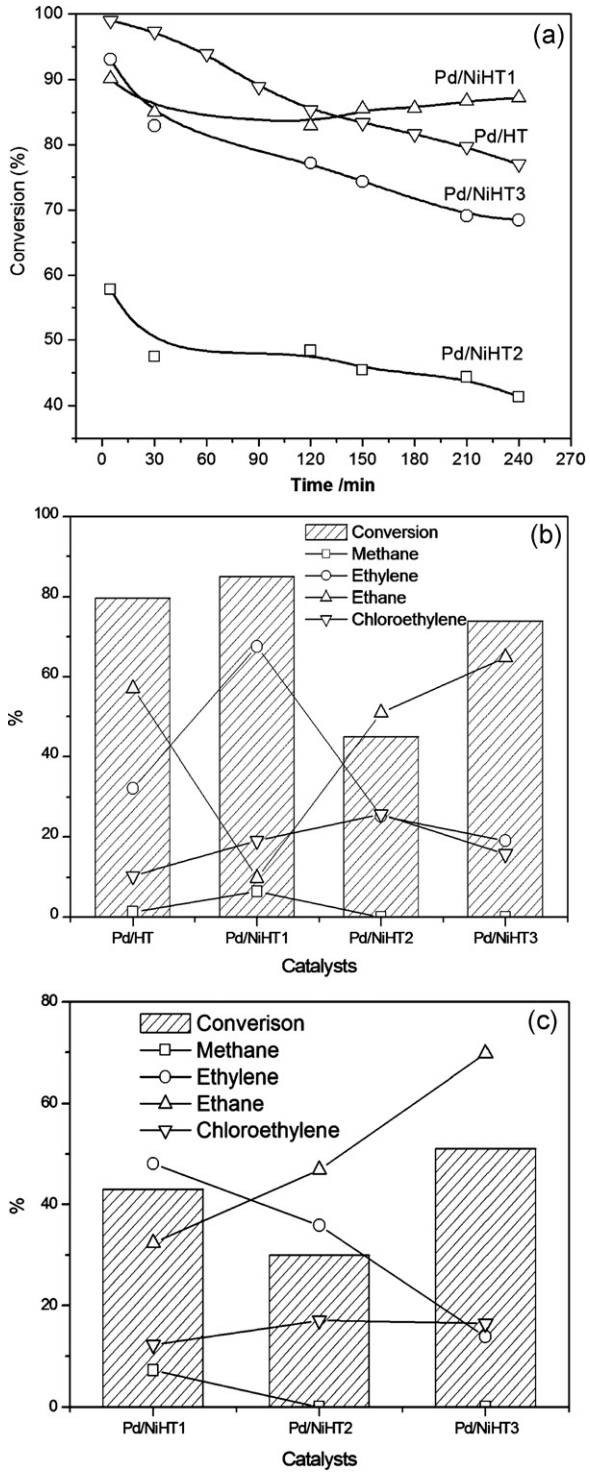

Fig. 4. (a) Catalytic activity of Pd/HT and Pd/NiHT catalysts with different NiMgAl molar ratios (catalysts reduced at 623 K); (b) product distribution at high conversion; (c) selectivity at lower conversion level.

reaction. Moreover, since Ni has the ability to hydrodechlorinate, an increase in Ni content should also affect the catalytic activity, despite the low reducibility of the NiMgAl support at this temperature according to the H_2-TPR. At the same time, an increase in the Mg content in the support resulted in an improved catalytic activity, as shown for Pd/NiHT3. This can be explained by the metal-support cooperation, where the higher basicity of the support resulting from the Mg species promotes the Pd. This effect is clearly observed for the Pd/HT catalyst. In summary, the catalytic conversion follows a trend of Pd/HT > Pd/NiHT1 > Pd/NiHT3 > Pd/NiHT2.

The product distribution over these catalysts at the end of the reaction (i.e. after 240 min on stream, as obtained from Fig. 4a) is displayed in Fig. 4b. In addition, the selectivities were compared at low conversion levels (Fig. 4c). For this, the space velocity was increased three times without changing the H_2/TCE molar ratio. During the catalytic reaction, ethylene, ethane and chloroethylene (CE) were the main products, though methane, 1,1-dichloroethylene and 1,2-dichloroethylene (DCE) were also detected. At the end of the reaction, the highest ethylene selectivity was obtained over Pd/NiHT1, whereas Pd/NiHT3 and Pd/HT samples exhibited a higher selectivity to ethane. Fig. 4c summarizes the selectivity of the catalysts reduced at 623 K at lower initial conversion levels. A similar trend in selectivity was observed as in Fig. 4b, where the Ni-rich Pd/NiHT1 catalyst favored mainly formation of ethylene (47%) with 32% ethane selectivity, while the Mg-rich Pd/NiHT3 catalyst mainly produced ethane (66%) with only 13% ethylene selectivity. Overall, the selectivity of the catalysts towards ethylene formation follows a trend: Pd/NiHT1 > Pd/NiHT2 > Pd/NiHT3. From the above results it is tempting to conclude that, the lower the Pd/Ni ratio is, the higher is the ethylene selectivity, whereas upon increasing the Pd/Ni ratio, i.e. more metallic Pd is at the surface, a higher ethane production was observed. Carefully analyzing the above results, a significant amount of ethane (>30%) was formed on Pd/NiHT1 catalyst despite the low Pd/Ni metal ratio on the surface. This shows the direct involvement of metallic Pd in the hydrodechlorination reaction. From H_2-TPR analysis, no reduction of NiO was initiated at temperature lower than 700 K. This suggests generally that the Pd/NiHT catalysts reduced at 623 K contain mainly metallic Pd and small amounts of metallic Ni species. Consequently, their catalytic activity is mainly governed by the noble metal, which is responsible for hydrogenation of the ethylene to ethane. Comparing the three catalysts, Pd/NiHT1 catalyst showed higher ethylene selectivity. This could be related to the reducibility of NiO in the catalysts, which increases from NiHT3 < NiHT2 < NiHT1. Thus, the Pd/NiHT1 is expected to involve more metallic Ni species accounting for the difference in ethylene selectivity among the different supports. This is further corroborated by formation of small amounts of methane observed on Pd/NiHT1, which most likely occurs on reduced Ni sites. Hence, in order to investigate the role and catalytic properties of the Ni, a higher catalyst reduction temperature was employed for the Ni rich catalyst.

3.2.2. *Effect of the reduction temperature*

The effect of the catalyst reduction temperature on the catalyst performance was studied for the gas phase HDC reaction of TCE. The NiHT1 catalyst was selected for this test due to its better performance at lower reduction temperature compared to the others. Fig. 5 shows the catalytic behavior of the NiHT1 catalyst reduced at 623 K, 723 K and 823 K in flowing hydrogen. A clear tendency is observed. An increase in the reduction temperature improved the conversion from 32% to 63%, as shown in Fig. 5a.

Ethylene, methane, CE and traces of DCE were the products detected over NiHT1 after applying different reduction temperatures (Fig. 5b). The production of ethylene and methane increases at higher reduction temperature. In fact, the increase in methane production is associated with the ability of Ni for the C—C bond cleavage at high temperatures. On the other hand, a decrease in vinyl chloride formation was observed as the reduction temperature increased. Here it is important to note that small amounts of ethane were detected only for the catalyst reduced at the highest temperature.

Indeed, under conditions of HDC, three processes can occur over Ni surfaces. Nickel is generally known for its ability to

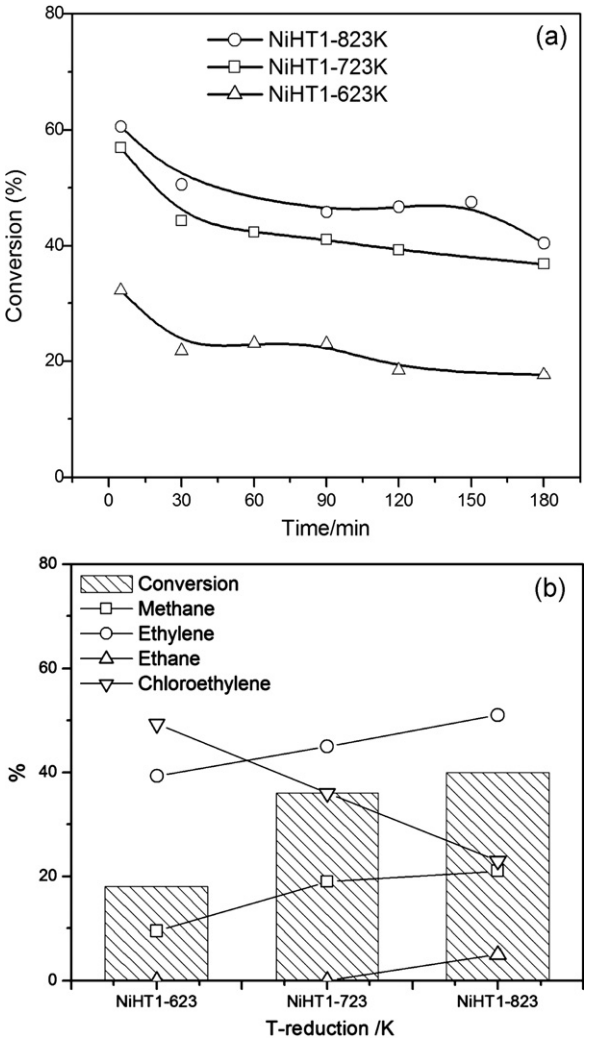

Fig. 5. Effect of the reduction temperature on the catalytic properties of NiHT1 catalysts: (a) conversion, (b) product distribution at 180 min reaction time.

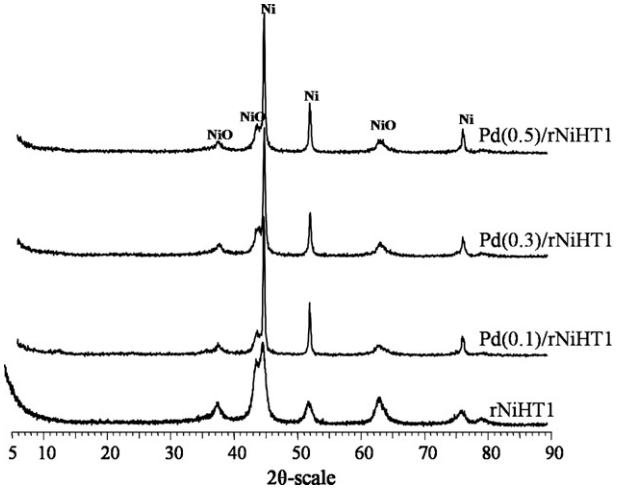

Fig. 6. X-ray diffraction patterns for rNiHT1 and Pd/rNiHT1 catalysts.

catalyze hydrogenation, hydrogenolysis and hydrodechlorination processes. During hydrodechlorination of TCE, ethane can be formed by hydrogenation of ethylene and can further undergo hydrogenolysis to form methane. The changes in selectivity observed for NiHT catalysts, when the reduction temperature is increased, may be attributed to the migration of reduced Ni from the bulk of the mixed oxide to the surface. The hydrodechlorination of the C—Cl bond may require large particle ensembles, and high temperature reduction likely generates a number of sufficiently large Ni clusters favoring the C—Cl bond scission [1,2]. The hydrogenolysis ability of NiHT catalysts for C—C bond cleavage (formation of methane) seems to be also induced by the high temperature reduction.

In conclusion, with increasing reduction temperature the concentration of metallic Ni in the NiHT1 sample also increased. This promotes both the conversion and the selectivity to ethylene. Thus, the NiHT1 catalyst is favorable for selective HDC of TCE to ethylene. Despite the higher selectivity to ethylene for the NiHT1 catalyst, the HDC activity (<60%) is relatively low. The HDC ability can be enhanced by the addition of palladium, as described in this work, thereby improving the conversion and stability of the catalyst, without significantly affecting the selectivity to ethylene. Noble metal catalysts are considered to be highly active for the HDC reaction, but present low selectivity towards formation of ethylene. Addition of a small amount of Pd enriches the Ni catalyst with sufficient active hydrogen and hence promotes the HDC reaction.

3.2.3. *Effect of the Pd incorporation protocol*

A different catalyst synthesis protocol was adopted and its effect on the HDC performance was tested. The synthesis protocol allows the evaluation of the influence of the metal–metal interaction between Pd and Ni at the surface. In this synthesis protocol, palladium was impregnated over pre-reduced (823 K) NiHT1 catalyst. The resulting Pd/rNiHT1 catalyst was reduced prior to the reaction at 623 K. A higher reduction temperature (823 K) was employed in order to induce the migration of the reduced Ni species from the bulk of the mixed oxide to the surface.

The X-ray diffraction profiles for Pd/rNiHT1 catalysts are displayed in Fig. 6. Reflections corresponding to metallic Ni species (JCPDS-03-065-2865), periclase (JCPDS-87-0653) or NiO (JCPDS-00-044-1159) phases were detected. Reflections corresponding to Pd or Pd-Ni alloy species were not observed either due to the small Pd loading or due to the high dispersion over the surface of the rNiHT1 catalyst, or due to masking by metallic Ni.

Low-magnification HRTEM images of samples with 0.1, 0.3 and 0.5 wt.% of Pd are shown in Fig. 7a, b and c, respectively. All samples are very similar and comprised by small particles of about 5–15 nm in size, as expected for NiMgAl oxides derived from NiMgAl hydrotalcites. Fig. 7(d) corresponds to a HRTEM image of sample with 0.3 wt.% of Pd along with the corresponding Fourier transform (FT) image. Rings at 1.49, 2.11 and 2.43 Å match exactly the (2 2 0), (2 0 0) and (1 1 1) crystallographic planes of MgO, respectively. In addition, spots at 1.76 Å correspond well to the (2 0 0) spacing of metallic Ni. The location of MgO and Ni in the image has been indicated with appropriate labels. In this sample, as well as in the sample with 0.1 wt.% of Pd, Pd or Pd-bearing particles are elusive, possibly due to the low amount of Pd. Therefore, more effort has been invested in the analysis of the sample with the highest Pd loading (0.5 wt.%). In this sample, metallic Ni as well as Ni-Pd particles has been identified (see Fig. 7e and f). Fig. 7e shows a crystallite with lattice spacing at 2.04 Å, which corresponds to the (1 1 1) crystallographic planes of metallic Ni. Lattice fringes are perfectly defined and no defects are detected. In contrast, Fig. 8f shows another particle with a particular microstructure, as deduced from the accurate analysis of its lattice fringes. Different contrast areas are identified in the HRTEM image with different lattice fringes, as revealed by their profile analysis. Areas with lattice fringes at 2.16 Å alternate with brighter areas with lattice fringes at 2.04 Å. As explained above, lattice fringes at 2.04 Å correspond to (1 1 1) crystallographic

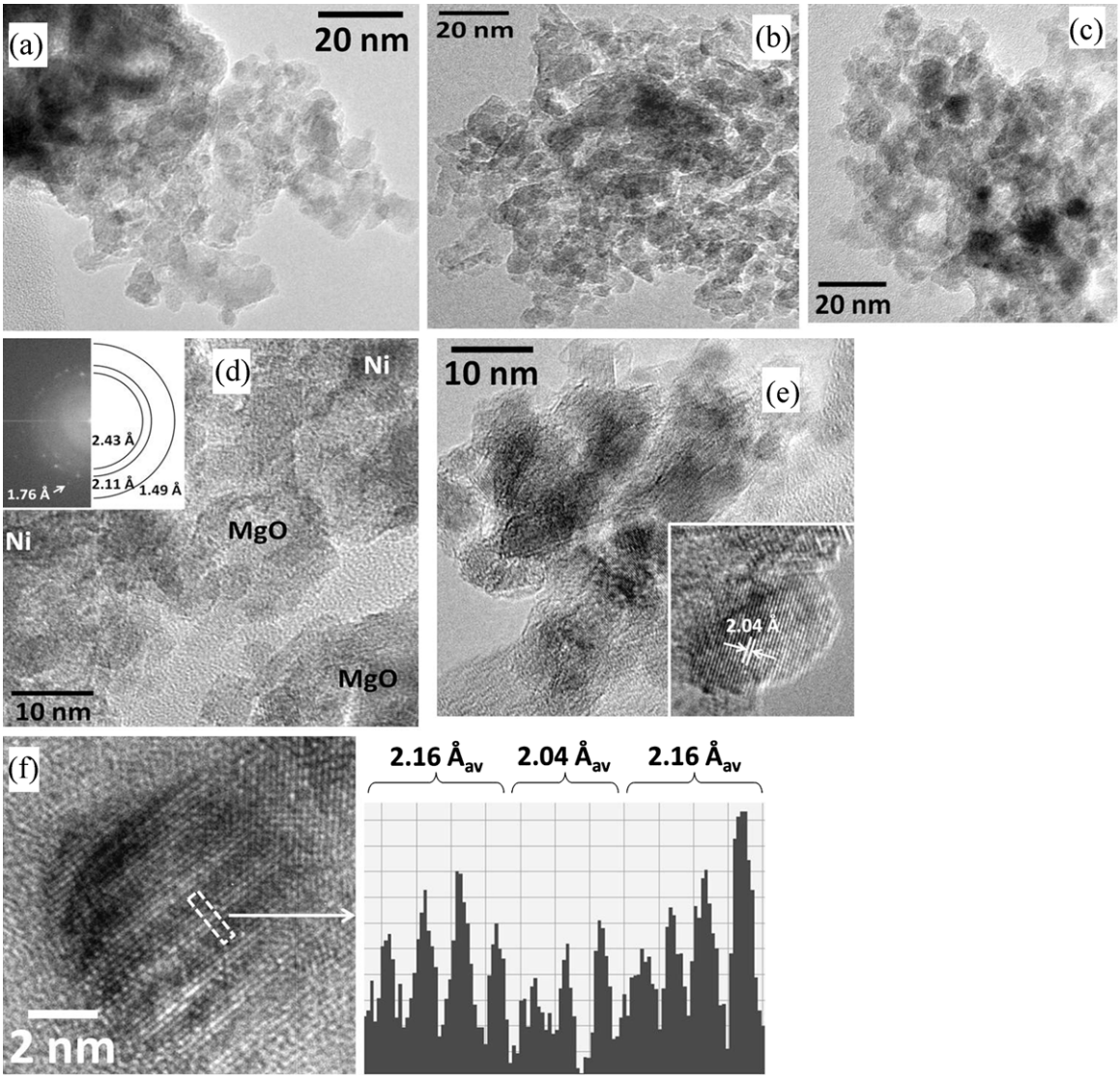

Fig. 7. Low and high magnification TEM images of Pd/rNiHT1 catalysts.

planes of metallic Ni, but the new lattice fringes at 2.16 Å are intermediate of (1 1 1) planes of Ni at 2.04 Å and (1 1 1) planes of Pd at 2.25 Å. Taking into account that both metallic Ni and Pd exhibit the Fm3m crystallographic structure, it is likely the formation of an Ni-Pd alloy.

Fig. 8a compares the catalytic activities of Pd/rNiHT1 and Pd/NiHT1-623 catalysts. HDC of TCE over Pd/NiHT1-623 catalyst resulted in 90% initial conversion. Pd(0.5)/rNiHT1, Pd(0.3)/rNiHT1 and Pd(0.1)/rNiHT1 reached an initial conversion of 89%, 87% and 82%, respectively. The Pd(0.1)/rNiHT1 catalyst showed more rapid deactivation than the others, most probably due to its lower Pd loading. Comparable catalytic activity was recorded for Pd/NiHT1-623 and Pd(0.5)/rNiHT1, which possess the same Pd loading.

Fig. 8b and c represent the selectivities at initial and end (i.e. after 180 min TOS) conversion levels from Fig. 8a, respectively. The main products observed during HDC of TCE were ethylene, methane, ethane, chloroethylene and traces of dichloroethylene. As shown in Fig. 8b and c, the selectivity of ethylene at initial and end conversion levels for Pd/NiHT1-623 catalyst was around 49% and 67%, respectively. Throughout the reaction an increase in ethylene selectivity and a decrease in ethane selectivity were observed. Higher selectivity to ethylene was observed for Pd(0.5)/rNiHT1 (about 66%) at initial conversion (see Fig. 8b). According to previous works [10] this synthesis protocol is likely to result in a better metal–metal interaction. Since the palladium was added after the support treatment at high reduction temperature (823 K), it is highly possible that the resultant surface of the Pd/rNiHT1 catalyst surface was better promoted by the Pd introduced. Higher ethylene selectivity at initial conversion on Pd(0.5)/rNiHT1 shows that the surface is probably enriched in metallic Ni in cooperation with a Pd-Ni alloy, which was detected by HRTEM. However, after 3 h of reaction time a drastic decrease in ethylene selectivity (23%) and an increase in ethane (64%) formation was observed for Pd(0.5)/rNiHT1 (Fig. 8c). A potential reason for the increasing hydrogenation of the double bond on Pd(0.5)/rNiHT1 with time on stream could be related to the segregation of Pd leading to increased ethane formation on the Pd. In a bimetallic system the component that interacts more strongly with the ambient gas can diffuse to the surface. For the Pd-Ni system, during reduction hydrogen is strongly adsorbed on the Pd surface, which may favor the enrichment of the surface with Pd [28]. This process could play a role with longer reaction times. At the beginning of the reaction the higher concentration of metallic Ni at the surface leads to a higher selectivity to ethylene. However, with increasing reaction time, Pd or Pd-Ni alloy may segregate to the surface and be involved directly in the ethane formation. In case of the Pd/NiHT1-623 catalyst stronger interaction of the oxide

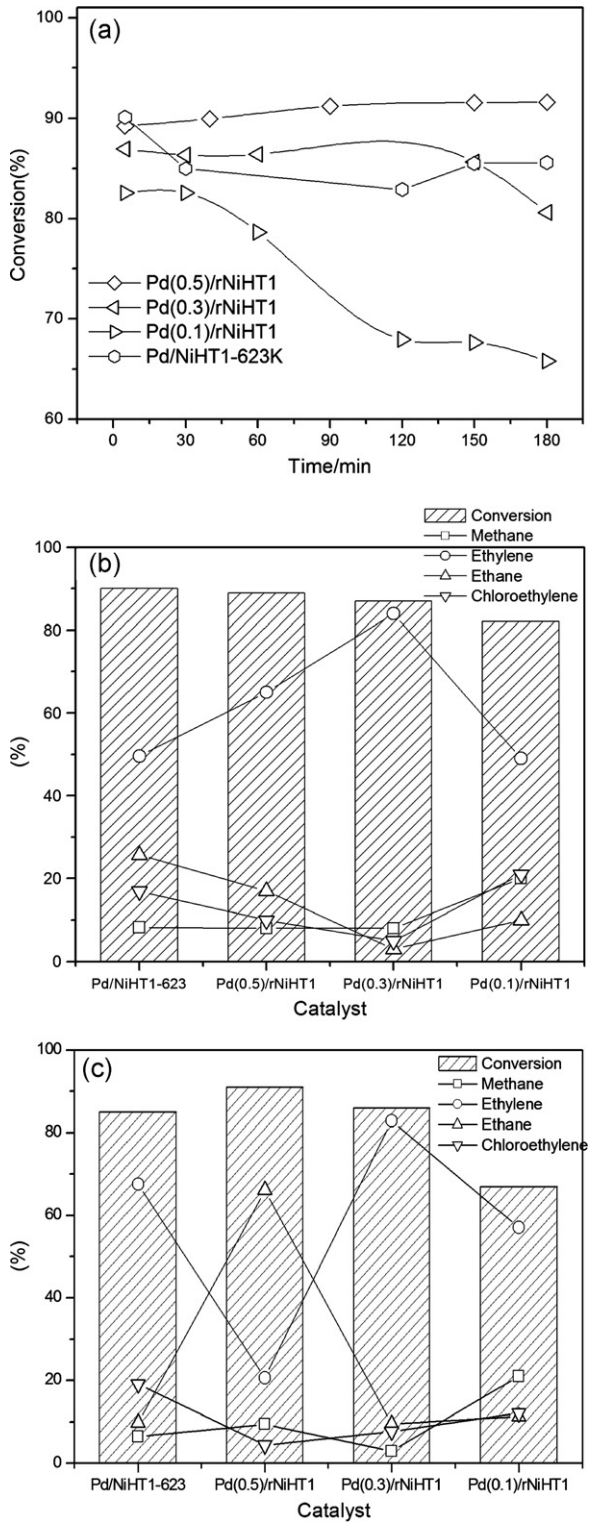

Fig. 8. (a) Conversion vs. reaction time for Pd/rNiHT1 and Pd/NiHT1-623 catalysts; (b) product distribution at the beginning of the reaction; and (c) product distribution after 3 h time on stream.

support with the Pd is expected. Due to the stronger interaction, Pd segregation is unlikely to occur, thus inhibiting the formation of ethane.

To improve the selectivity to ethylene with time on stream, while maintaining the higher catalytic activity of the Pd/rNiHT1 catalyst, a lower Pd loading was employed. Since Pd is responsible for hydrogenation of ethylene to ethane, lowering its amount could favor ethylene production. As expected, the initial catalytic activity of Pd/rNiHT1 slightly decreases as the Pd amount decreased. However, as shown in Fig. 8b and c, lowering the Pd loading to 0.3% drastically increased the ethylene selectivity (80%), at the same time maintaining an initial conversion level like that of Pd(0.5)/rNiHT1. After 3 h of catalytic testing, the selectivity of ethylene remained constant. Thus, the Pd(0.3)/rNiHT1 catalyst exhibited better catalytic activity and ethylene selectivity. Further lowering the Pd content to 0.1 wt.% decreased the catalytic activity to 82%, however, a lower selectivity to ethylene was found than over the 0.3 wt.% Pd catalyst. At the end of the reaction these catalysts showed an increase in methane and chloroethylene formation. In general, the selectivity towards ethylene formation at initial conversion follows a trend: Pd(0.3)/rNiHT1 > Pd(0.5)/rNiHT1 > Pd/NiHT1-623 K > Pd(0.1)/rNiHT1, and after 3 h of reaction: Pd(0.3)/rNiHT1 > Pd/NiHT1-623 K > Pd(0.1)/rNiHT1 > Pd(0.5)/rNiHT1.

4. Discussion

As shown in Table 1, the hydrogen uptake value for the different catalysts follows a trend as Pd/NiHT1 > Pd/NiHT2 > Pd/HT > Pd/NiHT3. The TEM measurements revealed a similar Pd particle size for all these samples (Table 1); however, the correspondent H_2 uptake values are different. This effect can be explained considering the contribution of nickel. As the amount of Ni inside the mixed oxide increases, the H_2 uptake of the catalyst also increases. Lower H_2-uptake values were recorded for Pd/HT and Pd/NiHT3. From these results, it can clearly be seen that the hydrogen chemisorption capacity of the catalysts is strongly influenced by the presence of nickel and by the presence of MgO. For instance, the catalyst containing a higher Ni content, Pd/NiHT1, resulted in higher H_2 uptake. On the other hand, when comparing catalysts Pd/NiHT2 and Pd/NiHT3 that contain the same amount of nickel, the increase in the magnesium content decreases the H_2 uptake.

In general, depending on the degree of metal–metal or metal-support interaction the HDC catalytic activity and the selectivity towards formation of ethylene or ethane can be modified. For instance in the HDC reaction of TCE, noble metals, like Pd, tend to convert trichloroethylene to fully hydrogenated products like ethane. In contrast, mild hydrogenation catalysts like Ni form ethylene or other unsaturated products but with low conversions. Bimetallic catalysts can achieve both enhanced catalytic activity and selectivity towards ethylene formation. As a result, the catalytic activity of Ni can be modified by the addition of a small amount of Pd. The Pd has the ability to easily dissociate molecular hydrogen and to provide active hydrogen (spillover) for the reaction to proceed, while Ni is engaged in the HDC process. Consequently, the Ni particles that are located near Pd are probably highly active.

Considering the TOF values presented in Table 1, Pd/NiHT3 and Pd/HT catalysts showed the highest TOF. These catalysts also contain the highest MgO amount. In addition, comparing Pd/NiHT1 and Pd/NiHT2 catalysts, the former resulted in a higher TOF. This indicates that the presence of a higher quantity of metallic Ni species in the mixed oxide, with higher hydrogen uptake capacity, increases the HDC reaction activity. These results indicate that two factors mainly govern the HDC catalytic activity of the catalysts. The first is the fraction of exposed Pd and Ni metal. The second is the presence of MgO species in the support. It seems that there has to be a compromise in terms of mixed oxide composition (NiO and MgO content) and thus between metallic functionality and support basicity (presence of MgO species) for optimizing the catalytic behavior.

As shown in Fig. 4, the Pd/NiHT1 catalyst containing a higher amount of Ni achieved the best catalytic performance and attained

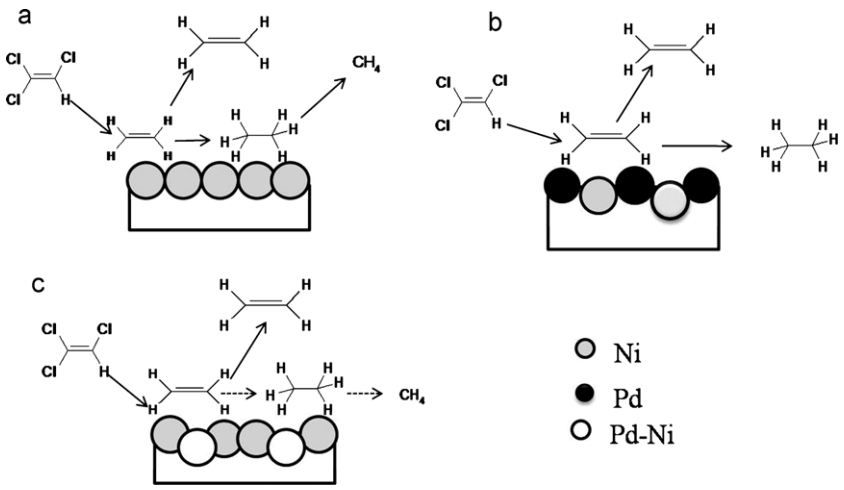

Scheme 1. Proposed pathway of ethylene conversion over Pd-Ni surfaces (dashed arrows represent less favored pathways).

a higher selectivity to ethylene. This implies that a catalyst containing a small amount of Pd deposited on a surface enriched with reduced metallic Ni favors the formation of olefinic products during HDC of TCE at 573 K. Another observation on Pd/NiHT catalysts with different Ni/Mg/Al ratios after reduction at 623 K is a significant formation of ethane apart from ethylene and other chlorinated hydrocarbons. The formation of ethane is likely to be favored over the surface of Pd despite its low metal loading. Hence, in the reaction, metallic Pd species are highly involved in the direct HDC of TCE to ethane and/or the hydrogenation of part of the formed ethylene to ethane. Application of a higher catalyst reduction temperature improved the catalytic activity of NiHT1. Ethylene, methane, and some chlorinated products were produced, while ethane was not detected. However, the formation of methane increased with the catalyst reduction temperature.

The proposed pathway for ethylene formation during HDC of TCE over reduced NiHT is displayed in Scheme 1a, based on the hypothesis that the formed ethane is rapidly transformed to methane. This can be further supported by two possible explanations. Since the activation energy required for hydrogenation of a double bond in unsaturated hydrocarbons is higher than that for the cleavage of the C—Cl bond [19,27], the dechlorination reaction over Ni catalysts might be faster than the further hydrogenation of ethylene in the hydrodechlorination of TCE. The second explanation is associated with rapid hydrogenolysis of ethane to methane at 623 K. The ethane produced by hydrogenation of ethylene could further be hydrogenated breaking the C—C bond. Scheme 1b shows the proposed pathway of the formation of ethylene during HDC of TCE over metallic Pd on NiHT, such as Pd/NiHT1-623 K. The TCE hydrodechlorinates finally to ethylene and chloroethylene, consequently the ethylene is hydrogenated to ethane by the Pd. The reduction treatment may generate a number of sufficiently large Ni clusters suitable for the C—Cl bond scission, as evidenced by the XRD analysis (Fig. 6). Bimetallic surfaces often exhibit compositions or structures that can deviate significantly from the bulk. The surface of a bimetallic system is usually enriched with the component with lower surface free energy. Surface segregation is a mechanism for lowering the overall surface energy. Considering that the surface free energy of Pd is lower than that of Ni, Pd preferentially enriches at the surface [28]. An additional parameter that may affect the surface composition is the selective chemisorption of a surrounding gas on the components of the bimetallic system. The component, which interacts more strongly with the ambient gas, could segregate to the surface. In the case of the Pd-Ni bimetallic system, both parameters lead to the enrichment of the surface with Pd. A better Pd-Ni interaction at the surface seems to be obtained by employing a different Pd incorporation protocol. On Pd(0.3)/rNiHT1, promotion of metallic Ni by the nearby Pd-Ni alloy, which was detected by HRTEM, improved the activity and selectivity to ethylene formation. The proposed mechanism of ethylene hydrogenation over this catalyst is depicted in Scheme 1c.

The deactivation observed for the catalysts during the HDC reaction could be related to the presence of chloride species, coking or metal sintering. For HDC reactions, the deactivation behavior usually depends on the operation conditions. It is well known that, during the hydrodechlorination reaction of chlorinated compounds using supported metal catalysts, the chloride species formed during the reaction can interact with the metallic and basic sites of the catalyst leading to deactivation [29–31]. Considering the experimental conditions, the main sources of deactivation in the HDC reaction are most probably the blocking of active sites by carbonaceous deposits and the presence of chloride species on the basic sites of the catalysts [23,31].

Comparing the stability of the NiHT1 catalysts reduced at different temperatures, the deactivation is highly pronounced for the catalyst reduced at lower temperature (623 K). This is probably due to the lower quantity of metallic Ni on the catalyst surface, which likely inhibits the formation of enough spill-over hydrogen responsible for self-regeneration of the catalyst. From this we can conclude that increasing the concentration of metallic Ni at the surface increases the stability of the catalyst.

Furthermore, the addition of a small amount of Pd to the NiHT1 catalyst improved significantly the stability in the reaction, as shown in Figs. 4a and 5a, when comparing Pd/NiHT1 and NiHT1-623 K. Since the formation of spillover hydrogen is promoted by the presence of the noble metal, the increase in stability of the Pd/NiHT1 catalyst is reasonable. This was further reinforced by the data presented in Fig. 8a, where an increase of the Pd content improved the stability of the catalysts against deactivation. The ability of Pd and Ni to form higher quantities of spillover hydrogen responsible for self-regeneration of the catalyst is the main factor for the catalysts stability. A similar conclusion was drawn by some of us [10] for Pd-Cu/Al_2O_3 catalysts applied in the same reaction.

5. Conclusion

Different Pd/NiMgAl catalysts were prepared and applied for gas phase HDC of TCE. The catalysts were activated using different catalyst reduction temperatures. Our findings demonstrate that NiMg(Al)O supported palladium catalysts are effective for

the gas phase hydrodechlorination of trichloroethylene. The catalysts performance for the hydrodechlorination was significantly affected by the Ni/Mg/Al molar ratio, the temperature of reduction, and the protocol of noble metal deposition onto the support. The selectivity towards ethylene formation increased with the concentration of surface metallic Ni formed upon high temperature reduction. Introduction of 0.5 wt.% Pd increased the catalytic activity. Higher ethylene selectivity (80%) was attained when Pd (0.3 wt.%) was introduced over already reduced NiHT mixed oxide. The method of Pd deposition affected the ability towards ethylene formation. Impregnation of Pd over previously reduced NiMgAl catalyst is an effective strategy to achieve better Pd-Ni interaction, enhancing the catalyst selectivity towards ethylene formation.

Acknowledgments

This work was financially supported by the MEC Spain and Austrian Exchange Service (Acciones Integradas, ES 05/2009), the Generalitat de Catalunya (ICREA ACADEMIA award) and the Marie Curie project (PIEF-GA-2009-236741 – ENVIROCATHYDRO).

References

[1] F.J. Urbano, J.M. Marinas, J. Mol. Catal. A: Chem. 173 (2001) 329–345.
[2] V.I. Kovalchuk, J.L. d'Itri, Appl. Catal. A: Gen. 271 (2004) 13–25.
[3] S. Ordóñez, F.V. Díez, H. Sastre, Ind. Eng. Chem. Res. 41 (2002) 505–511.
[4] S. Ordóñez, H. Sastre, F.V. Díez, Appl. Catal. B: Environ. 25 (2000) 49–58.
[5] S. Lambert, F. Ferauche, A. Brasseur, J. Pirard, B. Heinrichs, Catal. Today 100 (2005) 283–289.
[6] F. Alonso, I.P. Beletskaya, M. Yus, Chem. Rev. 102 (2002) 4009–4092.
[7] E. Matisová, S. Škrabáková, J. Chromatogr. A 707 (1995) 145–179.
[8] S. Kovenklioglu, Z. Cao, D. Shah, R.J. Farrauto, E.N. Balko, AIChE J. 38 (1992) 1003–1012.
[9] B. Heinrichs, F. Noville, J. Schoebrechts, J. Pirard, J. Catal. 220 (2003) 215–225.
[10] N. Barrabes, D. Cornado, K. Foettinger, A. Dafinov, J. Llorca, F. Medina, G. Rupprechter, J. Catal. 263 (2009) 239–246.
[11] W.D. Rhodes, K. Lázár, V.I. Kovalchuk, J.L. d'Itri, J. Catal. 211 (2002) 173–182.
[12] M. Martino, R. Rosal, H. Sastre, F.V. Díez, Appl. Catal. B: Environ. 20 (1999) 301–307.
[13] D.I. Kim, D.T. Allen, Ind. Eng. Chem. Res. 36 (1997) 3019–3026.
[14] P. Kim, H. Kim, J.B. Joo, W. Kim, I.K. Song, J. Yi, J. Mol. Catal. A: Chem. 256 (2006) 178–183.
[15] A.H. Weiss, S. Valinski, G.V. Antoshin, J. Catal. 74 (1982) 136–143.
[16] A. Śrębowata, W. Juszczyk, Z. Kaszkur, J.W. Sobczak, L. Kępiński, Z. Karpiński, Appl. Catal. A: Gen. 319 (2007) 181–192.
[17] S. Ordóñez, F.V. Díez, H. Sastre, Appl. Catal. B: Environ. 31 (2001) 113–122.
[18] Y.H. Choi, W.Y. Lee, J. Mol. Catal. A: Chem. 174 (2001) 193–204.
[19] Y. Choi, W. Lee, Catal. Lett. 67 (2000) 155–161.
[20] B. Aristizábal, C.A. González, I. Barrio, M. Montes, C. Montes de Correa, J. Mol. Catal. A: Chem. 222 (2004) 189–198.
[21] A. Śrębowata, W. Juszczyk, Z. Kaszkur, Z. Karpiński, Catal. Today 124 (2007) 28–35.
[22] V. Simagina, V. Likholobov, G. Bergeret, M.T. Gimenez, A. Renouprez, Appl. Catal. B: Environ. 40 (2003) 293–304.
[23] B.T. Meshesha, R.J. Chimentão, F. Medina, J.E. Sueiras, Y. Cesteros, P. Salagre, F. Figueras, Appl. Catal. B: Environ. 87 (2009) 70–77.
[24] Y. Cesteros, P. Salagre, F. Medina, J.E. Sueiras, D. Tichit, B. Coq, Appl. Catal. B: Environ. 32 (2001) 25–35.
[25] M. Boudart, H.S. Hwang, J. Catal. 39 (1975) 44–52.
[26] K. Schulze, W. Makowski, R. Chyzy, R. Dziembaj, G. Geismar, Appl. Clay Sci. 18 (2001) 59–69.
[27] B. Coq, J.M. Cognion, F. Figueras, D. Tournigant, J. Mol. Catal. A: Chem. 141 (1993) 21–33.
[28] A. Renouprez, J.F. Faudon, J. Massardier, J.L. Rousset, P. Delichère, G. Bergeret, J. Catal. 170 (1997) 181–190.
[29] S.I. Fujita, B.M. Bhanage, D. Aoki, Y. Ochiaia, N. Iwasa, M. Arai, Appl. Catal. A 313 (2006) 151.
[30] G. Del Angel, J.L. Benitez, J. Mol. Catal. A: Chem. 165 (2001) 9–13.
[31] B.T. Meshesha, R.J. Chimentao, A.M. Segarra, J. Llorca, F. Medina, B. Coq, J.E. Sueiras, Appl. Catal. B: Environ. 105 (2011) 361–372.